Title

Spinal cord interneurons are identified with pseudorabies viral injections into hindlimb muscles of spinal rats treated with olfactory ensheathing cells and epidural stimulation

Author

Tierno, Alexa Marie

Publication Date

2020

Peer reviewed|Thesis/dissertation

UNIVERSITY OF CALIFORNIA

Los Angeles

Spinal cord interneurons are identified with pseudorabies viral injections into hindlimb muscles of spinal rats treated with olfactory ensheathing cells and epidural stimulation

A thesis submitted in partial satisfaction of the requirements for the degree Master of Science in Physiological Science

by

Alexa Marie Tierno

2020

ABSTRACT OF THE THESIS

Spinal cord interneurons are identified with pseudorabies viral injections into hindlimb muscles of spinal rats treated with olfactory ensheathing cells and epidural stimulation

by

Alexa Marie Tierno

Master of Science in Physiological Science

University of California, Los Angeles, 2020

Professor Patricia Emory Phelps, Chair

Transplantation of olfactory bulb-derived olfactory ensheathing cells (OECs) is a promising therapy to facilitate the regrowth of axons and promote functional recovery following injury. This study combines OEC transplantation and epidural stimulation during a climbing task following a severe transection of the thoracic spinal cord of inbred Fischer 344 rats. To examine propriospinal connectivity of axons across the injury site, we injected two strains of a transsynaptic retrograde tracer, pseudorabies virus (PRV); GFP-PRV was injected into the tibialis anterior of one rat hindlimb and RFP-PRV was injected into the soleus of the other. We analyzed the PRV-labeled neurons in the lumbar spinal cord to evaluate the extent of each PRV injection and to detect populations of cholinergic and Pax2-expressing PRV-labeled interneurons. Several dually infected PRV interneurons from antagonistic muscles were detected in the lumbar cord. We also found that there were more Pax2-expressing PRV-labeled interneurons in media- compared to OEC- or fibroblast-treated rats. Next, we looked at the injury site block and found that many rats displayed incomplete lesions and that a proportion of PRV-

labeled neurons above the lesion site are V2a or cholinergic interneurons. In addition, we located PRV-labeled neurons several segments above the injury site in a location and distribution characteristic of sympathetic preganglionic neurons. PRV-labeled V2a interneurons were detected near sympathetic preganglionic neurons, as well as in the intermediate thoracic spinal cord. Overall, our results demonstrate that tissue sparing may facilitate regeneration or reorganization of propriospinal circuits following injury after cellular transplantation and epidural stimulation.

The thesis of Alexa Marie Tierno is approved.

Stephanie Ann White

Victor R. Edgerton

Patricia Emory Phelps, Committee Chair

University of California, Los Angeles

2020

TABLE OF CONTENTS

LIST OF FIGURES

Introduction

Spinal cord injury (SCI) often results in the loss of motor function below the lesion site. Following injury, axon regeneration across a severe or complete spinal cord transection is difficult due to the inhibitory environment created around the injury site. Several treatments targeted to overcome this challenge have shown promising results. Specifically, olfactory ensheathing cell (OEC) transplantation into the spinal cord of injured rats promoted modest functional recovery (Ramón-Cueto et al., 2000; Takeoka et al., 2011). In their native environment, peripheral OECs in the lamina propria surround axons of olfactory sensory neurons as they extend from the olfactory epithelium and through the cribriform plate. The axons of olfactory sensory neurons then associate with central OECs in the olfactory nerve layer of the olfactory bulb as they course to their targets (Li et al., 2005). When transplanted into the spinal cord, olfactory bulb-derived OECs modify the injury site by reducing the amount of tissue damage, interacting with the glial scar to form astroglial bridges on which axons can grow into the injury site, and suppressing chondroitin sulfate proteoglycans and immune cell activation and infiltration (Khankan et al., 2016).

Another promising therapeutic treatment geared towards restoration of locomotor function following SCI is epidural stimulation (Gad et al., 2013). During development, axons are dependent on activity for their growth and survival, including the stabilization of dendrites and synapses (Mennerick and Zorumski, 2000). Thus, stimulation of the spinal cord below the site of injury can facilitate the growth of axons and recovery of hindlimb function (Mondello et al., 2014). While the epidural stimulation is effective, its combination with an activity potentiates its therapeutic capability. For example, stimulation of the lumbar spinal cord after a complete spinal cord transection can facilitate stepping movements when combined with weight bearing and

stepping on a treadmill (Courtine et al., 2009; Edgerton and Harkema 2011; Harkema et al., 2011). A combination of epidural stimulation, climb training, and OEC transplantation may therefore lead to greater anatomical and functional recovery than these individual treatments alone.

To determine if there is anatomical evidence of axons crossing the lesion site, a transsynaptic retrograde tracer, pseudorabies virus (PRV), was injected into one hindlimb muscle per leg of the severely transected, inbred Fischer 344 rats at 5.5-6.5 months post-injury. Specifically, we wanted to identify the types of interneuron populations labeled with the virus at this time post-injury. We first quantified the extent of PRV within the somatic motor neurons in the lumbar spinal cord, the neurons that transport the virus into the CNS. Then, we looked for populations of lumbar interneurons, including cholinergic interneurons, such as the medial partition or central canal cluster cells, and Pax2-expressing cells. Next, we asked if the virus was detected directly above the lesion site, and if so, what types of cells were labeled. Neuronal populations examined included the excitatory V2a interneurons, characterized by their expression of the transcription factor Chx10 (Crone et al., 2008; Thornton et al., 2018) and cholinergic neurons. Finally, we looked further rostrally, several segments above the lesion site, for any evidence of PRV-labeled neurons that were either cholinergic or expressed Chx10.

Material and Methods

Implantation of stimulating and electromyography (EMG) recording electrodes

Partial laminectomies were performed at spinal levels L2 and S1 and epidural stimulating electrodes were placed on the dorsal dura mater and attached to a headplug, as reported in

Thornton et al. (2018). Surgical EMG implantation methods were similar to those in Gad et al. (2013). EMG electrodes were placed in the soleus and tibialis anterior (TA) muscles bilaterally. Following two weeks of recovery, rats began climb training while receiving sub-threshold (95%) epidural stimulation for 20 min/day, 3x/week for 5.5 or 6.5 months.

Spinal cord injury and cell transplantation

Inbred Fischer 344 rats (Charles River, SAS-FISCH) were given a severe mid-thoracic spinal cord transection three weeks after electrode implants using one of two methods: a microaspiration method for the F1 cohort and a microscissor cut for the F2 cohort. The final F1 cohort (n = 9) had a partial laminectomy performed at T7-T9 and a small incision was made in the dorsal dura, leaving the rest of the dura intact. Scissors were inserted and the spinal cord was cut at two sites spaced 1 mm apart. A sterile glass pipette tip connected to a surgical vacuum tube was inserted through the incision to extract the spinal cord tissue. The F2 cohort (n = 10) was given a transection at T7/T8 using microscissors, leaving the ventral and lateral dura mostly intact (Thornton et al., 2018). OECs from the olfactory bulbs of eGFP-expressing Fischer 344 rats (RRRC P40OD011062, University of Missouri) were cultured and purified as in Khankan et al. (2016). Skin biopsies from the abdominal walls of eGFP-expressing rats were dissociated into fibroblast (FB) cultures as previously reported (Khankan et al., 2016) and used as control transplanted cells for the F2 cohort. Fourteen days after injury, either media alone (n = 5; F1 cohort), media with FBs (n = 6; F2 cohort) or media with OECs (n = 8; F1 and F2 cohorts) was transplanted rostral, within, and caudal to the injury site. For OEC or FB transplants, serum-free Dulbecco's Modified Eagle Media (DMEM, Life Technologies #11995-065) containing calpain

inhibitor (MDL28170, 50 mM, Sigma #M6690) was injected into the spinal stumps. Cells transplanted at the injury site were suspended in fibrinogen (25 mg/ml, Sigma # F6755), thrombin (25 U/ml, Sigma #T5772), and a calpain inhibitor, forming a temporary fibrous matrix. Media controls received injections of DMEM in fibrinogen and thrombin with the calpain inhibitor into the lesion core and DMEM containing the calpain inhibitor into the spinal stumps.

PRV injections

At 5.5 or 6.5 months post-injury for the F1 and F2 cohorts, respectively, rats received an injection of eGFP-expressing PRV Bartha-152 and RFP-expressing PRV Bartha-614 (generous gift from Drs. Patrick Card and Lynn Enquist, Center for Neuroanatomy of Neurotropic Viruses). eGFP-expressing PRV was injected into the tibialis anterior (8 injections of 2.5 µL, 1.21×10^{9} pfu/mL) while RFP-expressing PRV was injected into the contralateral soleus (4 injections of 2.5 µL, 9.05×10^{8} pfu/mL). These two strains of PRV have similar infection and transport rates and have been used in dual-infection studies previously (Banfield et al., 2003). The sides of the injections varied for each rat. PRV injections were performed as described in Thornton et al. (2018). Rats were perfused 5 or 5.5 days after the PRV injections in the F1 and F2 cohorts, respectively.

Tissue preparation

Rats were deeply anesthetized with intraperitoneal injections of ketamine (90 mg/kg) and xylazine (10 mg/kg) and perfused intracardially with 4% paraformaldehyde-lysine-periodate (4%

PLP). Tissue was post-fixed in 4% PLP for 3 hours (Card and Enquist, 2014). Spinal cords were dissected, placed in 30% sucrose for 2-3 days, and embedded in OCT (Fisher #4585). Spinal cords at the injury site (T7-T11) and most lumbar levels L2-L6 were sectioned sagittally at 25 μm and sections were mounted in series onto 16 slides so that each slide contained a representative 6-7 sections, each 400 μm apart. Thoracic sections above the lesion site (T3-T6) and some lumbar level blocks were sectioned horizontally and mounted using the method described above. Slides were stored at 4°C in Millonigs buffer with 0.06% azide.

Immunohistochemistry

To assess somatic motor neurons infected by PRV, we used standard fluorescent immunohistochemistry to localize choline acetyltransferase (anti-ChAT, 1:500, Millipore, AB144P) in lumbar (L2-L6) spinal cord sections together with either anti-red fluorescent protein (RFP, 1:500, rabbit, Abcam, # AB62341) or anti-green fluorescent protein (GFP, 1:1000, chicken, Aves Labs Inc., Cat.# GFP-1020). Slides were rinsed with 0.1 M Tris buffer containing 1.4% NaCl and 0.1% BSA, followed by 5% normal donkey serum (NDS, Jackson ImmunoResearch Laboratories, #017-000-121) for an hour prior to incubation of the ChAT antibody for 2 nights, followed by a one-night incubation of the other two primary antibodies. To visualize the antibody labeling, slides were incubated with species-appropriate AlexaFluor 488, 555, and 647 (1:200-500, Jackson ImmunoReseach Laboratories) secondary antibodies and counterstained with bis-benzimide (1:500, Sigma-Aldrich, # B2261). To reduce background, spinal cord sections were then treated with TrueBlack Lipofuscin Autofluorescence Quencher (1:20 in 70% EtOH for 1 min; Biotium, #23007), followed by a quick buffer rinse, and then

coverslipped with Everbrite mounting medium (Biotium, #23001). Identical methods were performed on thoracic (T3-T6) spinal cord sections to assess cholinergic interneurons labeled with PRV above the lesion site.

We used standard fluorescent immunohistochemistry protocols to identify V2a or cholinergic interneurons near the injury site (T7-T11). The following primary antibodies were used: 1) Anti-Chx10 (1:1000, goat, Santa Cruz, # sc-21690) which identifies Chx10-positive V2a interneurons, or anti-ChAT to identify cholinergic interneurons 2) anti-Rb133 (1:7500, rabbit, gift from Dr. Enquist), which recognizes PRV structural proteins, 3) anti-GFP to detect the presence of GFP-positive OECs, FBs, or GFP-positive PRV infected cells, and 4) anti-glial fibrillary acidic protein (GFAP, 1:1000, mouse, BD Biosciences, #556327) to visualize astrocytes surrounding the lesion site. The Chx10 and ChAT primary antibodies were incubated for 2 nights, followed by an overnight incubation of the other primary antibodies. Slides were processed as before using the appropriate secondary antibodies for visualization. Similar methods were used for visualization of Chx10-expressing neurons above the lesion site at the thoracic (T3-T6) level of the spinal cord. Standard immunohistochemistry was used to visualize PRV-positive cells using GFP and RFP primary antibodies, together with the appropriate secondary antibodies and a nuclear counterstain. Sections were incubated with TrueBlack as described above before coverslipped.

To identify Pax2-expressing neurons, we used Tyramide Signal Amplification (TSA-Plus, PerkinElmer, # NEL741). Sections were rinsed with 0.1 M Tris buffer containing 1.4% NaCl and 0.05% Tween-20, followed by blocking using TNB and avidin-biotin-complex blocking solutions (1:1), and then incubated with anti-Pax2 (1:500, Zymed Laboratories, #71-6000) overnight. We used a biotinylated secondary antibody (1:500, donkey-anti-rabbit, Jackson

ImmunoReseach Laboratories, #711-065-152), streptavidin horseradish peroxidase (1:250, PerkinElmer, # FP1047), and cyanine-5 fluorophore diluted in amplification buffer (1:150, PerkinElmer, # FP1171). Before a second rabbit antiserum was used, sections were fixed in 4% paraformaldehyde for 15 min, rinsed, and heated in 10 mM citric acid buffer (pH 6.0), followed by three 10-minute rinses before incubation with the second rabbit antisera (anti-Rb-133). Standard immunohistochemistry was then used to visualize PRV-positive cells using anti-GFP. Slides were processed as before using the appropriate secondary antibodies for visualization and a nuclear counterstain, followed by TrueBlack incubation.

Image Acquisition

Panorama images were acquired using an Olympus AX70 microscope equipped with an AxioCam HRcRv.2 and ZEN software (2012, Zeiss). Confocal images were taken with a Zeiss Laser Scanning Microscope (LSM780) with solid-state lasers 488 nm, 561 nm, and 633 nm for triple-labeled images and 488 nm or 561 nm and 633 nm for double-labeled images. The 405 nm laser was used to image Hoechst as a nuclear marker or GFAP as a marker for astrocytes near the lesion site. Sections were captured with a 40x oil immersion lens (numerical aperture 1.3) or 63x oil immersion lens (numerical aperture 1.4) with the pinhole aperture set to 50 µm. Areas where cells above the lesion were located were scanned within the depth of the section where signals of all channels were detected to generate z-series of approximately 6-10 µm, with a z-separation of 1 µm. ZEN lite (v. 2.3) imaging software was used for all analyses. All optical sections per z-series were analyzed to confirm double-labeling. Images were psuedocolored, edited and compiled into figures with Adobe Photoshop.

Experimental design and statistical analyses

For somatic motor neuron and cholinergic interneuron quantification in L2-L6 spinal cord levels, 2 slides for each of the 19 rats were used. Each slide contained either 4-5 evenly-spaced, horizontal or 6-7 sagittal spinal cord sections. Somatic motor neurons were counted if labeled with RFP or GFP and ChAT in the ventral horns. PRV-positive cells were counted if a distinct cell soma and at least one process was observed. Cell counts were averaged between the two slides from the same side of the spinal cord processed for ChAT, RFP, and GFP to obtain a mean. The average cell counts per hemicord for each rat were analyzed by PRV injection (GFP-PRV or RFP-PRV) and reported as a mean ± SEM.

RFP- and GFP-PRV-labeled interneurons were counted in each spinal cord section per spinal rat and averaged between the two slides processed for ChAT, GFP, and RFP. We used a 10 μm diameter cutoff when counting PRV-positive cells as described in Thornton et al. (2018). Cells that appeared to be double labeled in the panoramic photomicrograph were confirmed by confocal microscopy. The percentage of RFP- or GFP-PRV-labeled interneurons out of total PRV-labeled interneurons in each animal was compared by location in the spinal cord (ipsilateral versus contralateral to muscle injection) and treatment group (OEC-, media- or FB-treated) and reported as mean percentage ± SEM.

For Pax2 analysis in L2-L6 spinal cord, one slide with 4-5 horizontal or 6-7 sagittal spinal cord sections was used for each of the 19 spinal rats. Pax2- and PRV-labeled neurons were counted and divided by the total number of PRV neurons per spinal rat to get a ratio of Pax2-PRV labeled neurons to total PRV-labeled neurons. Ratios were compared between transplant

treatment groups. To compare group means, a two-way ANOVA was used, followed by post hoc *t*-tests when differences were observed. Statistical significance was determined at $*p < 0.05$ and $**p < 0.01$.

Chx10 and PRV cells directly above the injury site (T7-T11) were quantified for all 19 rats using one slide from each rat, with 5-6 sagittal spinal cord sections. The slide adjacent to the one used for Chx10 analysis was used to quantify cholinergic interneurons. PRV-containing cells located above the injury site were reimaged with confocal microscopy to confirm double-labeling.

Quantification of Chx10- and ChAT-expressing cells labeled with PRV at T3-T6 spinal levels was conducted with one slide, each with a total of 4-5 horizontal spinal cord sections for all 19 rats. Cells that appeared to be labeled with PRV and Chx10 or PRV and ChAT were confirmed with confocal microscopy. Double-labeled neurons were counted and divided by the total number of PRV-labeled neurons in each section per spinal rat. Ratios were then averaged by treatment group or injury type (complete versus incomplete) and reported as mean percentages ± SEM.

Results

Somatic motor neurons and cholinergic interneurons in the lumbar spinal cord are retrogradely labeled with PRV

To evaluate the extent of PRV uptake by somatic motor neurons (SMNs), the lumbar spinal cord sections from each spinal rat were processed for choline acetyltransferase (ChAT), RFP-PRV

from injections into the soleus, and GFP-PRV for injection into the tibialis anterior (TA). We combined the F1 and F2 cohorts and found that 18 out of 19 rats showed evidence of SMN labeling with both RFP-PRV and GFP-PRV. One rat showed only RFP-PRV SMN labeling. As seen in Figure 1, a subset of somatic motor neurons were infected by RFP-PRV (arrows). There are a few RFP-PRV-labeled neurons that were weakly ChAT-positive within the motor pool (Fig. 1B, arrowhead), most likely due to the long virus exposure given that PRV-infected neurons can undergo cellular lysis in late stages of infection (Callaway, 2008; Thornton et al., 2018). The number of SMNs labeled with each virus varied between animals and even within individual animals, with a range of 11-77 SMNs labeled with either RFP- or GFP-PRV per spinal rat hemicord. Some animals exhibited more neurons labeled with GFP than with RFP (Fig. 2A-B), or vice-versa. There were no significant differences in the number of SMNs labeled by injections into the TA (GFP-PRV: 28 ± 3 SMNs) versus those into the soleus (RFP-PRV: 34 ± 5 SMNs). Thus, we confirmed that the virus was transported into the CNS from the soleus and TA muscles via SMNs.

Next, we examined the spinal interneurons labeled with the virus in the lumbar spinal cord. Rats with higher numbers of PRV-labeled SMNs had consistently more labeled interneurons compared to those rats with lower numbers of infected SMNs. Most PRV-labeled interneurons were found on the ipsilateral side of the PRV injection. In addition, 15 out of 18 rats with evidence of both viruses in the lumbar spinal cord had evidence of contralateral RFP-PRV and GFP-PRV neurons. In the other 3 rats, only one side of the spinal cord had contralaterally located RFP- or GFP-labeled neurons. Because all spinal rats had GFP-PRV injected into the tibialis anterior and RFP-PRV injected into the soleus, we asked if the number of contralaterally-located interneurons differed by muscle. There were no differences in the number of RFP- (8 ±

1.2%) and GFP-interneurons (7.8 ± 1.4%) located contralaterally. In addition, out of the 18 rats that showed transport of both viruses, 15 rats displayed neurons dually infected with GFP-PRV and RFP-PRV, indicating that these cells projected bilaterally (Fig. 3A-B, arrows and yellow arrowhead). No differences in the percentage of dually infected cells out of total PRV-labeled cells were found between OEC- (1.8 ± 0.6%), FB- (1.9 ± 0.7%), or media-treated (1.4 ± 0.7%) rats.

We also asked if ChAT-positive interneurons were labeled in the lumbar spinal cord. All 19 spinal rats showed evidence of PRV-labeled cholinergic interneurons. The two populations of cholinergic neurons labeled were the medial partition cells and central canal cluster cells (Phelps et al., 1984), and both are known to play a role in locomotion (Miles et al., 2007, Zagoraiou et al., 2009, Stepien et al., 2010, Tillakaratne et al., 2014). Here, we show that they contact SMNs directly or indirectly via a locomotor circuit related to the soleus and TA hindlimb muscles. Most of the PRV-labeled cholinergic cells were located ipsilateral to the side of injection, while a small number were detected contralaterally (Fig. 4A). Interestingly, there were cells that expressed both viral markers, in addition to ChAT (Fig. 3B, box C). Evidence of medial partition cells that expressed both GFP- and RFP-PRV (Fig. 3C, arrow) were found near the central canal. Other cholinergic interneurons were labeled with GFP-PRV (Fig. 4B1-2, arrow) or RFP-PRV (Fig. 4C1-2, arrow) and located ipsilateral to the muscle injection. We believe that some of these PRV-labeled cholinergic neurons are likely central canal cluster cells due to their size (about 25 μm in diameter) and proximity to the central canal (Phelps et al., 1984). Cholinergic interneurons that were labeled with PRV were typically surrounded by non-cholinergic PRV-expressing neurons and cholinergic neurons without PRV. Based on these data, cholinergic interneurons

make up a proportion of interneurons related to the locomotor circuitry of the TA and soleus in chronically-injured spinal rats.

A subset of Pax2-expressing neurons is detected with PRV in the lumbar spinal cord

To determine if there were inhibitory interneurons labeled with PRV in the lumbar spinal cord, we used Pax2, a transcription factor expressed by GABAergic and glycinergic neurons, to identify them (Batista and Lewis, 2008; Hori and Hoshino, 2012; Larsson, 2017). Most of the PRV-labeled Pax2-expressing neurons were found in laminae II-V of the dorsal horn in a sagittal section or intermediate grey matter in a horizontal section of the spinal cord, with either anti-GFP-PRV or anti-PRV alone (Fig. 5A and C). The GFP-PRV-labeled neurons (injection in the TA muscle) that co-expressed Pax2 (Fig. 5A, B1-3, arrows) were found mainly ipsilateral to the side of injection. Additionally, there were several PRV-labeled interneurons expressing Pax2 located medially, near the dorsal columns (Fig. 5C, D1-2, arrows) mixed with PRV-labeled interneurons that were Pax2-negative (Fig. 5C, D1-2, arrowheads). When the ratio of PRV-labeled cells that expressed Pax2 to total PRV-labeled cells was compared between OEC-treated rats and the controls, we found a significantly higher ratio in media-treated rats (38 ± 5%) as compared to FB- (15 ± 4%, $^{**}p=0.004$) and OEC-treated rats (14 ± 4%, $^{**}p=0.002$, Fig. 5E). This analysis found that the number of Pax2-expressing cells detected with PRV between FB- and OEC-transplanted animal groups did not differ.

Animals with incomplete injuries exhibit PRV labeling rostral to the lesion site

Now we examined the injury site (T7-T11) to determine the number of rats with PRV-labeled neurons located rostral to the lesion. Because the F1 and F2 cohorts had different transection methods, we treated the two groups separately. In the F1 cohort, 6/9 rats exhibited astrocyte bridges in the ventral spinal cord, suggestive of incomplete injuries. In this group, 2/4 OEC- and 4/5 media-treated rats had incomplete injuries, while the other 3 rats appeared to be completely transected. Rats in the F2 cohort received a micro-scissor transection, which yielded 9 out of 10 complete injuries with one FB-treated rat having a thin, continuous astrocyte bridge indicative of an incomplete injury site. All rats transplanted with OECs, regardless of cohort, showed OEC survival in the lesion core and/or the adjacent spinal cord stumps (Fig. 6A, inset). Of the 6 animals transplanted with FBs in the F2 cohort, 3 showed large clumps of surviving FBs, either rostral or caudal to the injury site.

To assess connectivity across the injury site, we looked for evidence of PRV-labeled neurons directly rostral to the lesion site in the spinal rats. In the F1 cohort, 2 OEC- and 3 media-treated rats had RFP-PRV-labeled neurons above the injury, and one of the media-treated rats displayed both RFP- and GFP-PRV-labeled neurons. The five rats with evidence of PRV above the lesion all had incomplete injuries, while the 4 rats without PRV above the lesion site were complete transections. In the F2 cohort, all 4 OEC- and 5/6 FB-treated rats had PRV labeling rostral to the injury site, with 8 rats showing both viral markers. The presence of PRV-marked neurons above the injury sites of incompletely transected rats suggests that even with small amounts of tissue sparing, the locomotor circuits can be modified by neurons above the injury.

Chx10-expressing neurons are labeled with PRV above the lesion site

To identify the types of neurons infected by PRV, we first examined V2a interneurons that are typically localized within the intermediate spinal cord (Al-Mosawie et al., 2007; Dougherty and Kiehn, 2010; Hayashi et al., 2018; Ni et al., 2014; Thornton et al., 2018). In this study, 2 OEC- and 2 media-treated rats in the F1 group and 2 OEC- and 2 FB-treated rats in the F2 group displayed PRV-labeled neurons that co-expressed Chx10 above the lesion site. One of the OEC-treated rats with a complete injury (Fig. 6A, asterisk) showed evidence of a GFP-PRV-expressing V2a interneuron (Fig. 6B1-3, arrow) located near a GFP-PRV-only expressing neuron (Fig. 6B1-3, arrowhead) rostral to the injury site. OEC-, media-, and FB-treated animals, however, displayed similar percentages of V2a interneurons expressing PRV out of total PRV neurons (15.6 ± 8.4%, 7.8 ± 4.8%, and 20.3 ± 16.3%, respectively).

We then looked for double-labeled PRV-Chx10 neurons in the T3-T6 spinal cord segments. Some PRV-labeled cells detected along the central canal co-expressed the V2a marker (Fig. 7A, A1-2, arrows). There was also evidence of V2a interneurons labeled with RFP- (Fig. 7B, B1-2, arrow) or GFP-PRV (Fig. 7C, C1-2, arrow) in the intermediate grey matter of the upper thoracic spinal cord and ipsilateral to the muscle injection. We counted the number of RFP- and GFP-PRV-labeled cells and then the number that co-expressed Chx10. Of those rats with PRV expression above the lesion, all 6 in the F1 cohort and 2/6 in the F2 cohort, exhibited double-labeled V2a interneurons. Most likely, the Chx10-expressing interneurons labeled with PRV contribute to the soleus and TA circuitry that persists following chronic SCI.

Most cholinergic neurons labeled with PRV above the injury site appear to be sympathetic preganglionic neurons

Due to the spinal transection level and distribution of PRV-labeled neurons, we suspected that the virus was transported from the blood vessel innervation of the muscle through the sympathetic chain ganglia. We therefore looked for groups of cholinergic PRV-labeled neurons in the injury site block (T7-T11) and found ChAT-positive, PRV-labeled neurons in 3 rats from the F1 cohort, 2 injected with OECs and 1 media control. The cholinergic, PRV-labeled neurons were located at least 3000 µm rostral to the injury site. As shown in Figure 8A and C, cholinergic neurons were found in the ventral and intermediate grey matter of the spinal cord above the lesion. The PRV-labeled cholinergic neurons were located in the intermediate grey matter (Fig. 8, arrows). In addition, cholinergic PRV-labeled neurons appear to express lower levels of ChAT compared to the surrounding PRV-negative cholinergic neurons (Fig. 8B and D, arrowheads). Based on their morphology, location, and ChAT expression, we identified these neurons as sympathetic preganglionic neurons (SPNs).

When we looked further rostrally at T3-T6 spinal cord levels, we found ChAT-positive PRV-labeled SPNs in the intermediolateral (IML) region of the spinal cord (Fig. 9A, B1-2, arrowheads). Together with ChAT-positive neurons, the PRV-labeled neurons had processes that characteristically extended rostro-caudally and medially. Some PRV-labeled neurons in the IML region appeared to be ChAT-negative, suggesting that those cells are dying or alternatively are interneurons that project to SPNs. In adjacent sections, we looked for V2a PRV-labeled interneurons and surprisingly found that some of the PRV-labeled neurons expressed Chx10 (Fig. 9C1-2, arrows). PRV was detected in 5/6 and 4/7 rats in the F1 and F2 cohorts, respectively, in the intermediolateral (IML) region above the lesion site. GFP-PRV injections

into the TA muscle resulted in 4 rats with ipsilateral GFP-labeled SPNs, while RFP-PRV injections into the soleus yielded 7 rats with ipsilateral RFP-labeled SPNs. Only 2/9 rats with PRV-labeled SPNs showed bilateral PRV transport via the sympathetic chain. Together, we conclude that PRV was transported through the locomotor circuitry via SMNs and through autonomic circuitry via the sympathetic chain ganglia in several of our spinal rats.

Discussion

In this study, we identified PRV-labeled SMNs associated with the TA and soleus muscles, along with populations of cholinergic, Pax2-positive, and V2a interneurons in the lumbar spinal cord. Surprisingly, some of the PRV-labeled interneurons in the lumbar spinal cord were labeled with both RFP- and GFP-PRV, and a small population were triple-labeled with ChAT. In addition, we found a greater proportion of Pax2-expressing interneurons labeled with PRV in media- than in OEC- or FB-treated rats. Many spinal rats in this study displayed incomplete injuries and V2a interneurons rostral to and several segments above their lesion site. We also found evidence of PRV-labeled SPNs above the lesion site in the IML and interestingly, V2a interneurons in this region were labeled as well.

Possible reorganization of circuitry below the lesion site

In the lumbar spinal cord, we found neurons labeled with both RFP-PRV from one hindlimb and GFP-PRV from the other. This viral expression pattern suggests that one neuron projects to both the soleus (extensor) and TA (flexor), antagonistic hindlimb muscles that are responsible for

opposing movements. Some of these dually-labeled neurons were also cholinergic and potentially represent a reorganization of the lumbar circuitry. Such connections are likely to be aberrant as Stepien et al. (2010) showed that cholinergic neurons located in this region project bilaterally, and preferentially contact functionally equivalent muscle groups rather than antagonists. It is possible that the epidural stimulation initiated a reorganization of circuitry at the lumbar level, as the electrodes stimulate the lumbosacral spinal cord of the injured rats (Gerasimenko et al., 2008; Ichiyama et al., 2008). Alternatively, the spinal cord injury itself may have altered these connections. Although we do not know the cause, this reorganization of cholinergic interneuron synapses onto motor neurons is likely to be non-functional. There may be other populations of double-labeled neurons that contact functionally antagonistic motor neuron pools bilaterally in the uninjured spinal cord.

PRV transport through sympathetic circuits

Previously, we reported that when PRV was injected into the soleus or TA of completely transected Sprague-Dawley rats 7 months after injury, there was viral labeling of ChAT-positive SPNs in the intermediolateral nucleus (IML) in 3/8 transected rats (Thornton et al., 2018). Here, we observed that over half of our rats had evidence of PRV in SPNs on one side of the spinal cord above the lesion site, consistent with previous retrograde labeling studies using PRV (Rotto-Percelay et al., 1992).

Interestingly, a few large, laterally located PRV-labeled cells near the SPNs were also labeled with the V2a interneuron marker, Chx10, in the upper thoracic area together with those in the intermediate grey matter. Studies using PRV as a method for labeling autonomic and

motor circuitry have demonstrated that there are supraspinal neurons that project to both SPNs and SMNs (Kerman et al., 2003). Following thoracic SCI, reportedly SPNs undergo morphological and synaptic changes due to the loss of supraspinal input (Krassioukov et al., 1999; Weaver et al., 1997). It is possible that the V2a interneurons we identified near the PRV-labeled SPNs may contact the PRV-labeled SPNs, suggesting transport through the sympathetic chain ganglion.

V2a interneurons play a role in functional recovery following injury

V2a interneurons are a glutamatergic population of neurons that project ipsilaterally, express Chx10, and are known to be involved with locomotion (Al-Mosawie et al., 2007, Crone et al., 2008; Dougherty and Kiehn, 2010; Hayashi et al., 2018). Specifically, ablation of these Chx10-positive neurons leads to disruptions in left-right coordination (Crone et al., 2008). Moreover, these neurons were suggested to make contacts with somatic motor neurons and commissural interneurons (Dougherty and Kiehn, 2010). In this study, we observed Chx10-positive cells that were infected with PRV rostral to the lesion in most incompletely transected spinal rats. Most Chx10-positive cells were found in the intermediate grey matter, which is where these neurons are reportedly concentrated (Hayashi et al., 2018; Ni et al., 2014). Recent studies reported that after a high cervical spinal cord injury, these Chx10-positive interneurons were recruited into the injured phrenic network (Zholudeva et al., 2017). Reorganization of local propriospinal networks may facilitate motor recovery following severe SCI (Courtine et al., 2008). We propose that the Chx10-positive, PRV-infected neurons identified rostral to the lesion site likely contribute to rearrangement of propriospinal circuits after SCI.

Our data suggest that in rats with incomplete injuries, propriospinal interneurons can form connections with the motor pools of the TA or soleus muscles. Cholinergic and inhibitory interneurons below the lesion site comprise a part of the locomotor circuitry which may be altered following injury in rats treated with epidural stimulation and climb training. Although it remains unclear if these treatments directly contribute to this reorganization or if this reorganization is functional, we have novel evidence showing that a variety of interneurons that constitute the locomotor circuits survive after chronic, complete or incomplete, spinal cord injury. Thus, the contributions of this study include identifying these interneuron populations in the lumbar region in adult rats with long-term severe spinal cord injuries treated with epidural stimulation, similar to treatments for people with chronic spinal cord injuries.

Figure Legends

Figure 1. Somatic motor neurons in the lumbar spinal cord are infected with pseudorabies virus expressing red fluorescent protein (RFP-PRV). A. Sagittal section of a lumbar spinal cord from a completely transected rat. Choline acetyltransferase (ChAT, white) was localized together with RFP-PRV (red, soleus muscle injection). B. B1-2: Enlargement from the inset in A shows that a subset of somatic motor neurons were infected with RFP-expressing PRV (arrows). Arrowheads point to a faintly RFP-labeled cell that appears to express ChAT and RFP at low levels. R: rostral, C; caudal, D: dorsal, V: ventral. Scale bars: A = 500 μm, B, B1-2 = 100 μm.

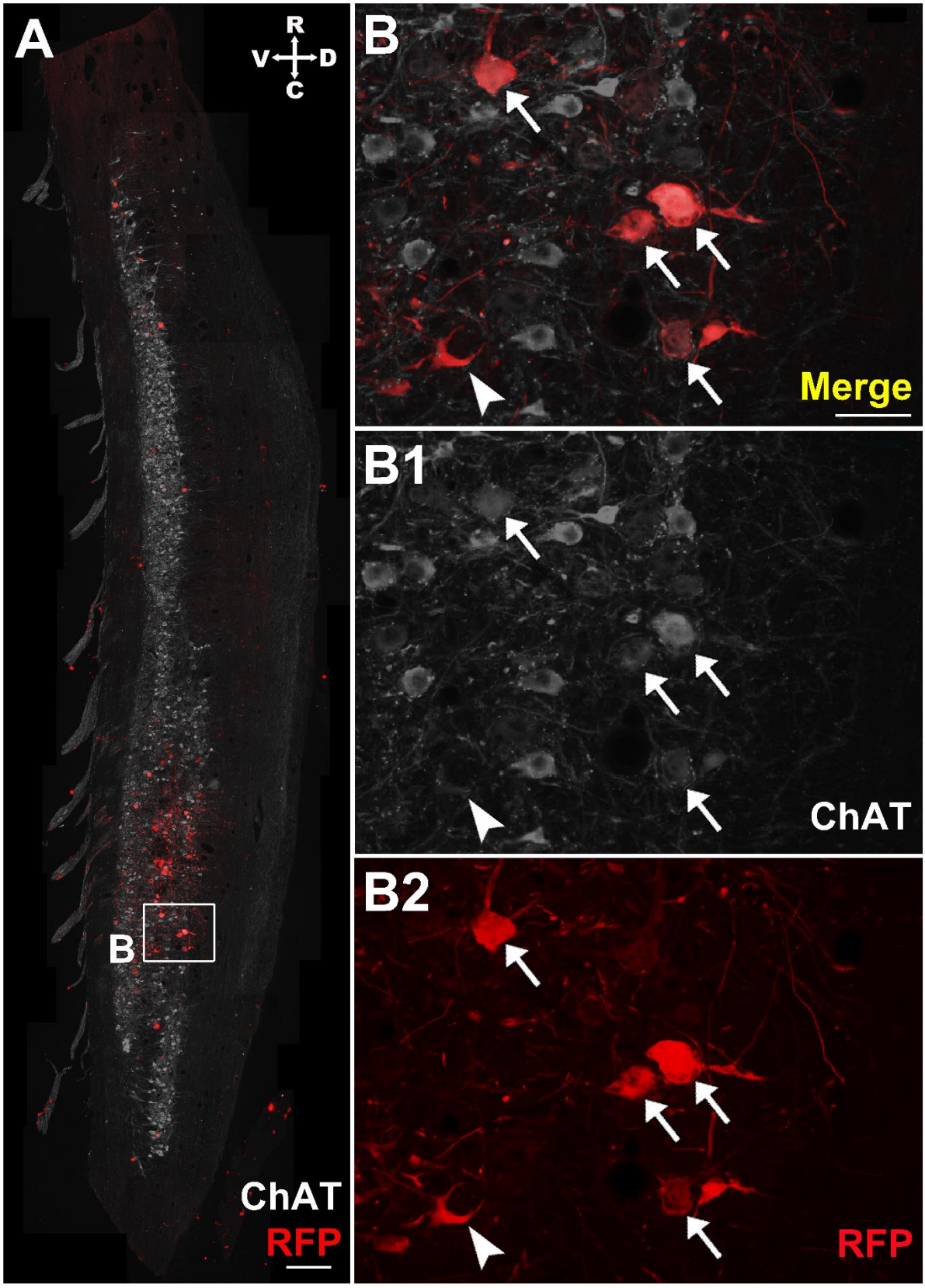
A
R
V
D
C
B
ChAT
RFP
B
Merge
B1
ChAT
B2
RFP

Figure 2. Spinal rats have different numbers of PRV-infected somatic motor neurons. Horizontal section of lumbar spinal cord from a spinal rat which was processed for RFP-PRV (red, soleus injection), and GFP-PRV (green, tibialis anterior injection) and ChAT (white). A, B. One side of spinal cord exhibits fewer somatic motor neurons that express RFP-PRV than the opposite side (B) that has more GFP-PRV-labeled motor neurons. R: rostral, C: caudal, L: lateral, M: medial. Scale bar A-B = 200 μm.

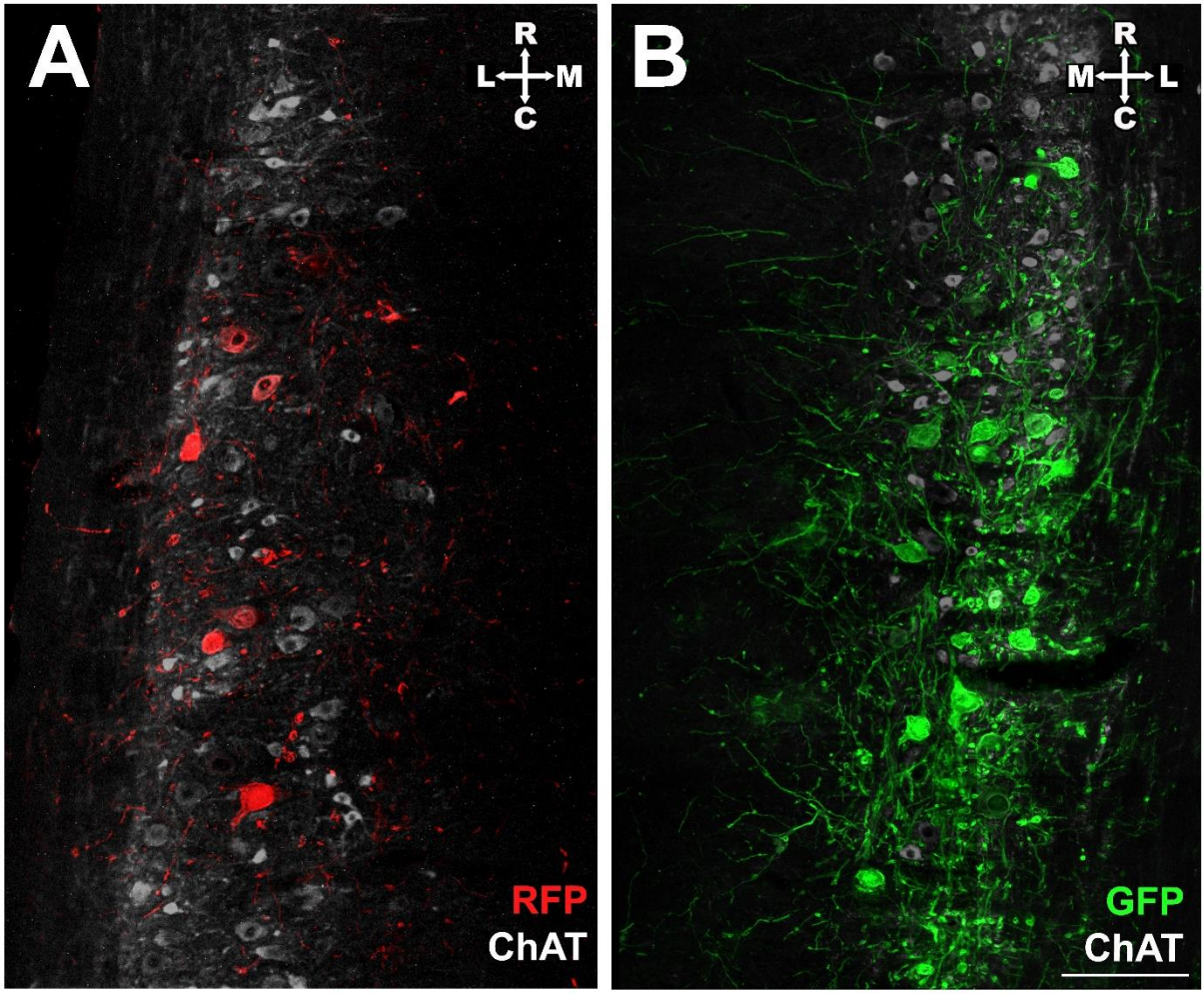
A
R
L
M
C
RFP
ChAT
B
R
M
L
C
GFP
ChAT

Figure 3. Interneurons in the lumbar spinal cord are dually labeled with RFP- and GFP-PRV and one is cholinergic. Confocal images of lumbar spinal cord display neurons identified with GFP-PRV (green, tibialis anterior) and RFP-PRV (red, soleus) injections and are located near the central canal. A, A1-3: Sagittal spinal cord section displays co-localized RFP- and GFP-labeled neurons (arrows) in the intermediate grey, just dorsal to the central canal. A single-labeled ChAT-positive neuron (white) is located nearby. B. Sagittal section contains many GFP-labeled ipsilaterally projecting neurons near the central canal (cc, marked by DAPI, blue), and a contralateral RFP-only cell (white arrowhead). A double-labeled RFP- and GFP-labeled cell (yellow arrowhead) was detected, together with a triple-labeled cell expressing GFP, RFP and ChAT (box C). C. C1-3: Boxed area in B shows a cholinergic interneuron labeled with both viruses. Based on size, location, and level of ChAT expression, this may be a medial partition cell. An RFP-PRV-labeled cell (arrowhead) is nearby. R: rostral, C: caudal, D: dorsal, V: ventral, L = lateral, cc = central canal. Scale bars: A, A1-3 = 20 μm, B = 100 μm, C, C1-3 = 50 μm.

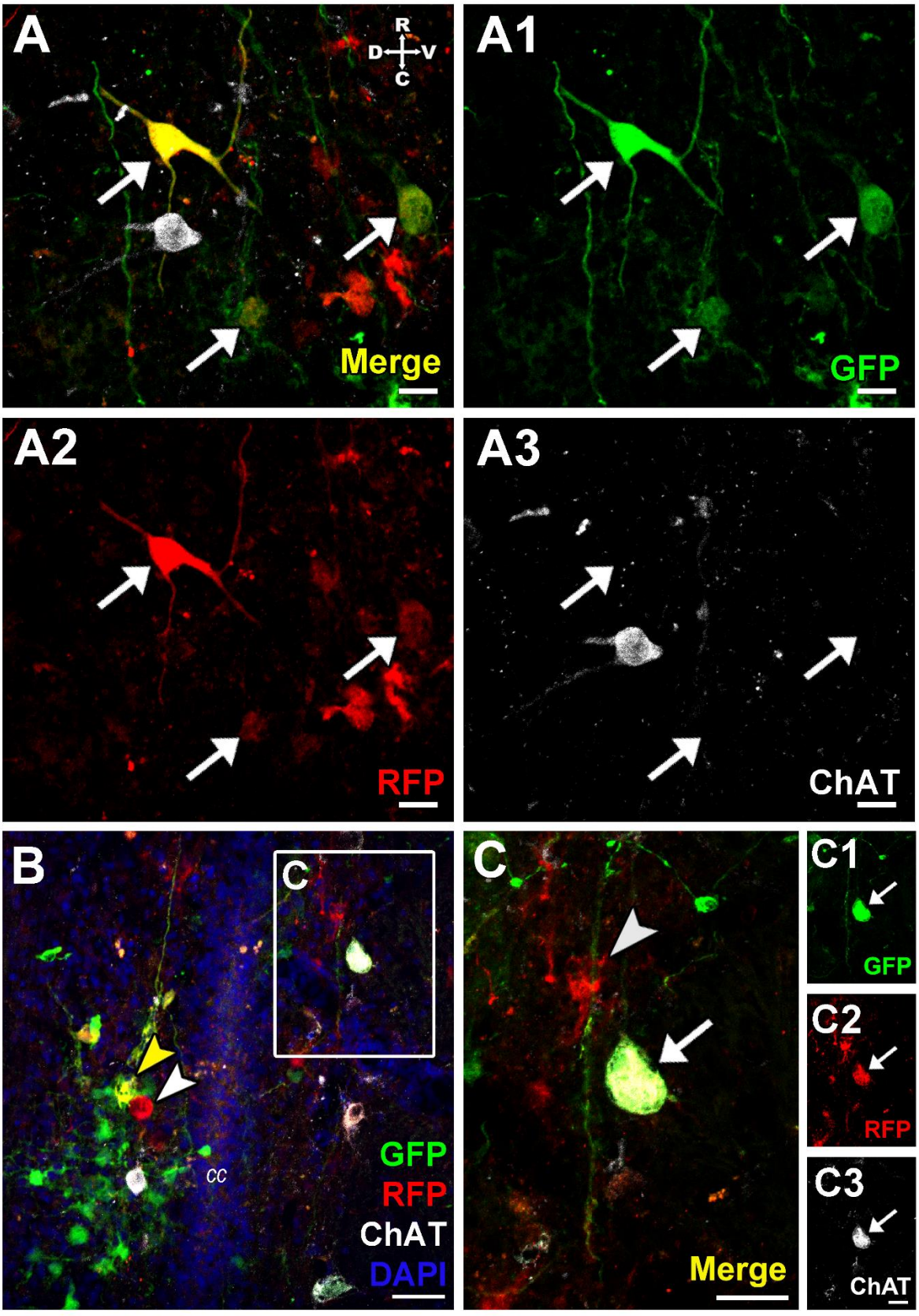
A
R
D
V
C
Merge
A1
GFP
A2
RFP
A3
ChAT
B
C
GFP
RFP
ChAT
DAPI
cc
C
Merge
C1
GFP
C2
RFP
C3
ChAT

Figure 4. PRV-labeled cholinergic interneurons are found in the lumbar spinal cord near the central canal. A. Horizontal lumbar spinal cord section with RFP-PRV (red, injected into the left soleus), GFP-PRV (green, injected into the right tibialis anterior), and ChAT (white) immunoreactivity. The RFP- and GFP-PRV-labeled neurons near the central canal are intermixed with small cholinergic interneurons. Several ChAT-labeled interneurons express GFP-PRV (box B) or RFP-PRV (box C). B. B1-2. A GFP-labeled cholinergic neuron (arrow) is located ipsilateral to the muscle injection and has a thick process that extends rostrally. C. C1-2. An RFP-PRV-expressing, small cholinergic neuron is found ipsilateral to the side of muscle injection and is near other cholinergic central canal cluster cells. R: rostral, C: caudal, L: left side, Ri: right side, cc: central canal. Scale bars: A = 100 μm, B, B1-2 and C, C1-2= 50 μm.

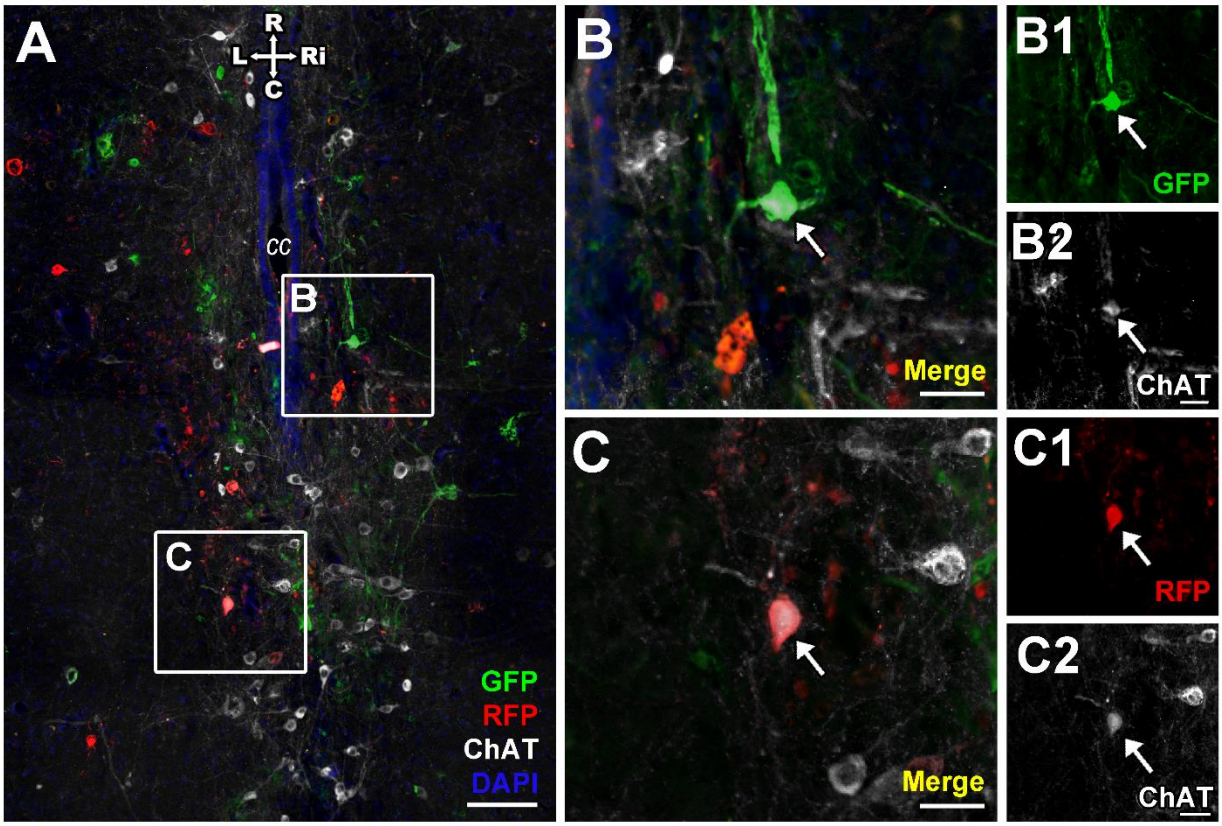
A
R
L
Ri
C
CC
B
C
GFP
RFP
ChAT
DAPI
B
Merge
B1
GFP
B2
ChAT
C
Merge
C1
RFP
C2
ChAT

Figure 5. Pax2-expressing dorsal interneurons are labeled with PRV in the lumbar spinal cord. A, B-B3. Sagittal lumbar spinal cord section was processed for PRV (red), GFP-PRV (green, ipsilateral tibialis anterior), and Pax2 (white) to identify PRV-labeled inhibitory interneurons. A. Lamina I of the dorsal horn is on the far left, and the ventral edge is on the far right. Some PRV-labeled neurons express Pax 2 (box B, arrows) in the dorsal horn, whereas others are Pax2-negative (arrowheads). B, B1-3: Enlargement of box B in A illustrates dorsal Pax2-expressing interneurons that contain PRV and GFP-PRV (arrows) from an ipsilateral tibialis anterior injection. C. Horizontal lumbar spinal cord section labeled with anti-PRV (red) and Pax2 (white). PRV-labelled cells are found on both sides of the dorsal columns (DC) in the deep dorsal horn. D, D1-2. Enlargement of box D from C illustrates two PRV-labeled neurons that express Pax2 (arrows) together with PRV-only neurons (arrowheads) and many Pax2-only cells. E. More Pax2-expressing cells were labeled with PRV in the lumbar spinal cord of media- than in OEC- or FB-treated rats (** $p < 0.01$). OEC-treated rats from the F1 and F2 cohorts were combined for this analysis. R: rostral, C: caudal, D: dorsal, V: ventral, L: lateral, DC: dorsal columns. Scale bars: A and C = 200 µm, B, B1-3 and D, D1-2 = 50 µm.

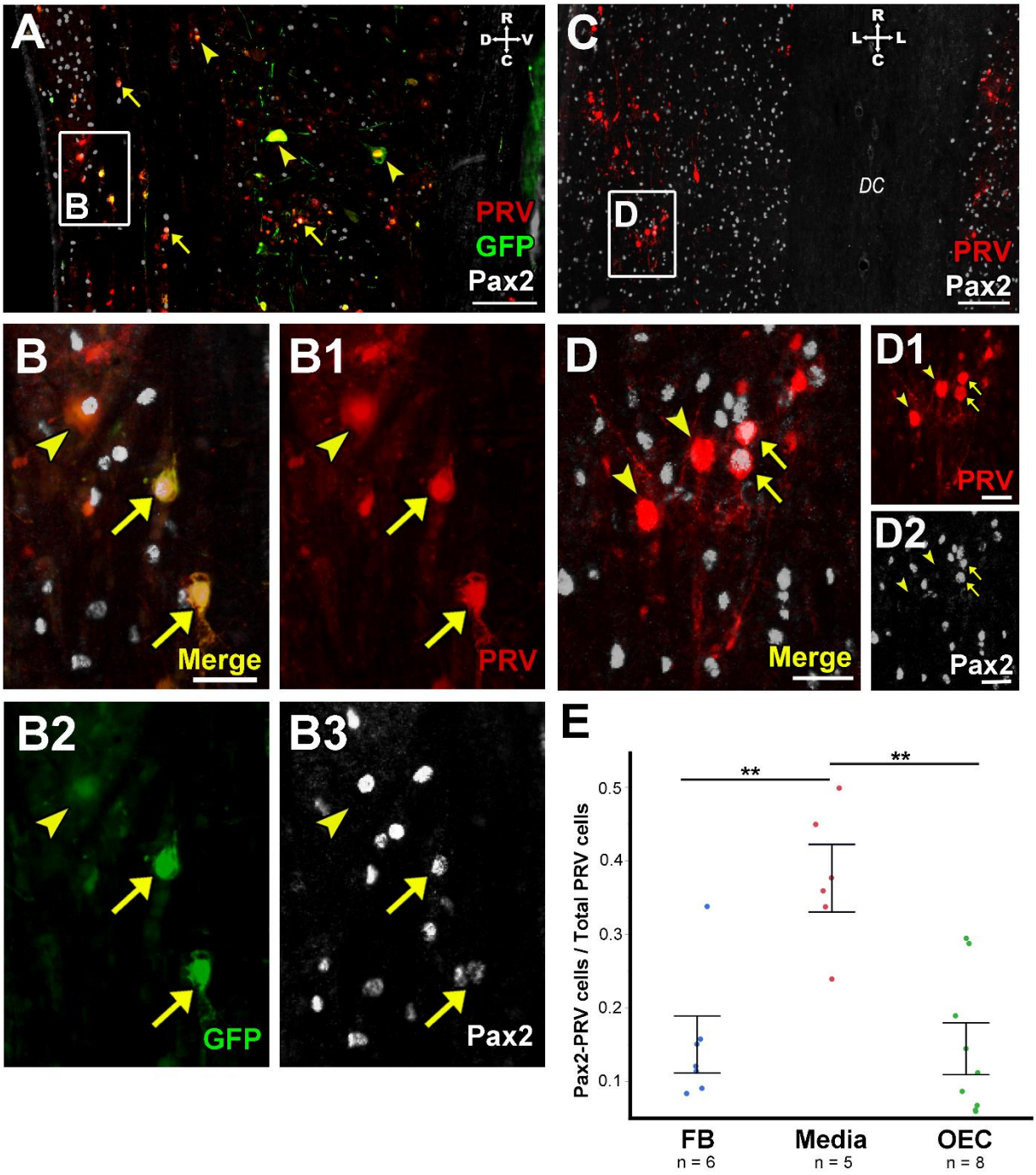
A
R
D
V
C
B
PRV
GFP
Pax2
C
R
L
L
C
DC
D
PRV
Pax2
B
Merge
B1
PRV
D
Merge
D1
PRV
D2
Pax2
B2
GFP
B3
Pax2
E
Pax2-PRV cells / Total PRV cells
0.5
0.4
0.3
0.2
0.1
**
**
FB
n = 6
Media
n = 5
OEC
n = 8

Figure 6. V2a interneurons labeled with PRV are found above the lesion site in a rat with a complete injury. A. Medially-located sagittal spinal cord section of an OEC-treated rat with a complete transection was labeled with anti-GFAP to delineate astrocytes (light blue), anti-PRV (red), anti-GFP-PRV (green) to identify infected neurons and GFP-expressing OECs, and anti-Chx10 to localize V2a interneurons (white). Inset shows surviving GFP-expressing OECs within the lesion core (*) of this spinal rat. B. B1-3: Confocal slice of box B in A shows two PRV- and GFP-labeled neurons, one of which expresses Chx10 (arrow) and other is Chx10-negative (arrowhead). R: rostral, C: caudal, D: dorsal, V: ventral. Scale bars: A = 500 μm, B, B1-3 = 10 μm.

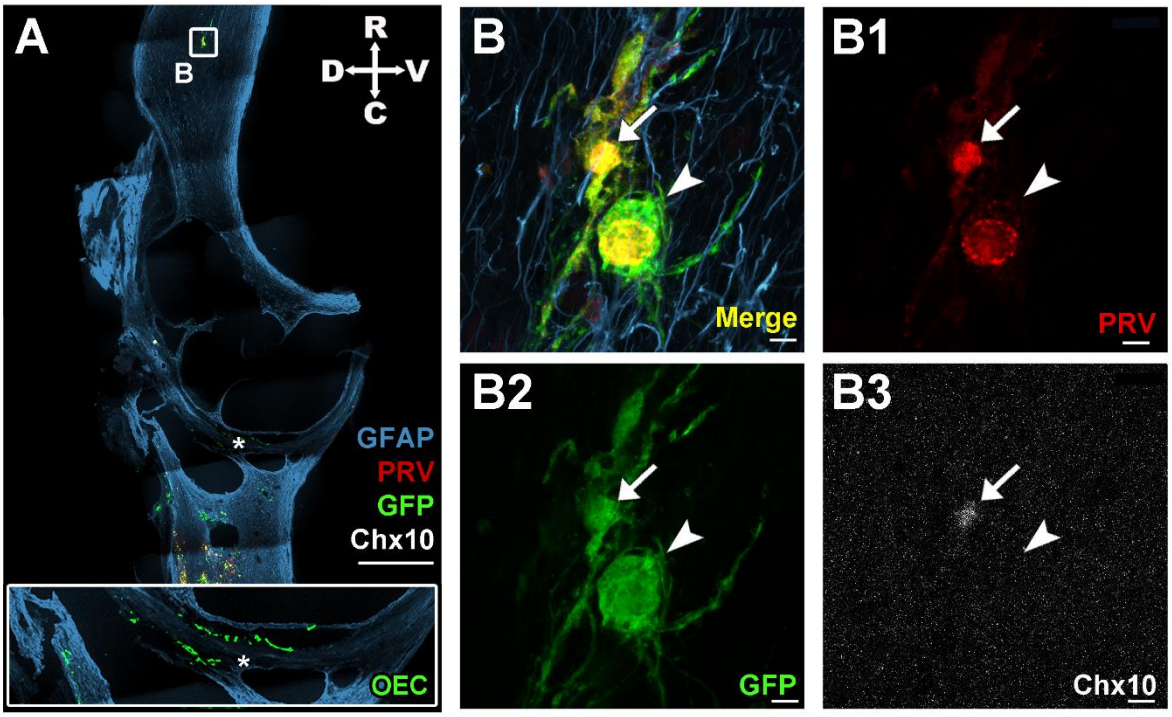
A
B
R
D
V
C
GFAP
PRV
GFP
Chx10
OEC
B
Merge
B1
PRV
B2
GFP
B3
Chx10

Figure 7. V2a interneurons are detected in horizontal sections several segments rostral to the injury sites of incompletely lesioned rats. A. A1-2: Thoracic (T3-T6) spinal cord section has RFP-positive cells (red, soleus injection) near the DAPI-labeled central canal (cc, blue). Some of these RFP-labeled cells express Chx10 (white; arrows), whereas others do not (arrowhead). B, B1-2: A large RFP-labeled neuron in the intermediate grey matter is ipsilateral to the muscle injection and co-expresses Chx10 (arrow). C, C1-2: A GFP-PRV-labeled neuron from the same rat shown in B is located on the opposite side in the intermediate grey and also expresses Chx10 (arrow). This double-labeled neuron is located ipsilateral to the tibialis anterior injection. R: rostral, C: caudal, L: lateral, cc: central canal. Scale bars: A = 200 μm, B and C = 100 μm.

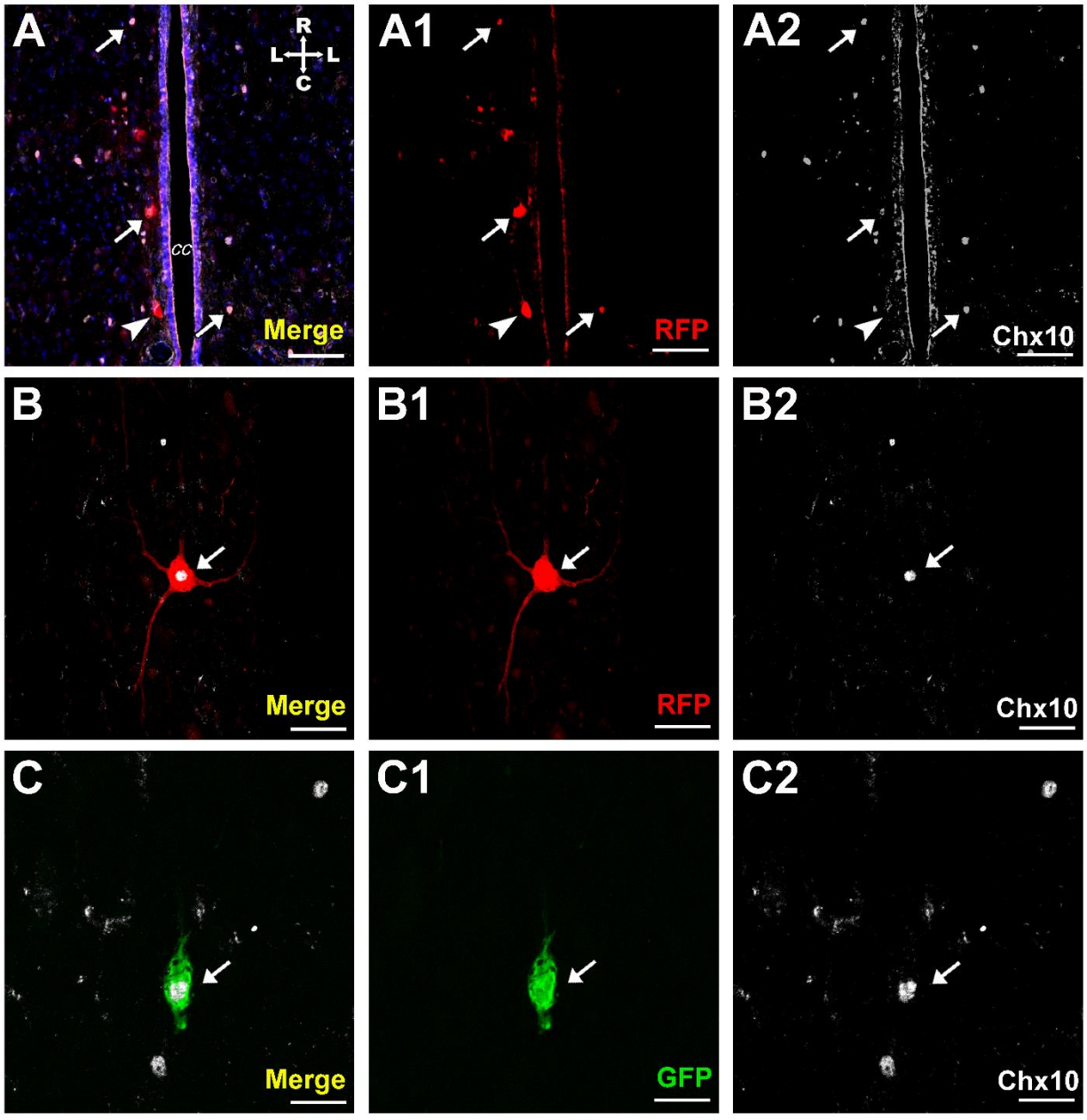
A
R
L
L
C
cc
Merge
A1
RFP
A2
Chx10
B
Merge
B1
RFP
B2
Chx10
C
Merge
C1
GFP
C2
Chx10

Figure 8. Sympathetic preganglionic neurons found above the injury sites of completely and incompletely lesioned rats. Sagittal spinal cord sections from the injury site block (T7-T11) were processed for anti-GFAP (light blue) to delineate astrocytes, anti-PRV (red) to localize PRV-labeled neurons above the lesion site, anti-GFP (green) to visualize GFP-PRV-labeled neurons and GFP-expressing OECs near the lesion, and anti-ChAT (white) to identify cholinergic neurons. A. Injury site from an incompletely transected, OEC-treated rat shows ChAT-positive somatic and sympathetic preganglionic neurons above the lesion, some of which are PRV-positive (boxed area). B. B1-2: High magnification confocal image of the box in A illustrates a cluster of cholinergic sympathetic preganglionic neurons (SPNs), one which is clearly labeled with PRV (arrow). Other PRV-labeled neurons (arrowheads) located near ChAT-positive neurons may be dying SPNs. C. Injury site of a fibroblast-treated rat displays a complete lesion and PRV-labeled neurons rostral to the lesion site (boxed area). Cholinergic neurons are found both in the ventral and intermediate grey matter. D, D1-3: Enlargement of confocal image from the box in C shows PRV-labeled neurons that also express low levels of ChAT (arrows) surrounded by high ChAT-expressing neurons. These are likely a group of SPNs. Other PRV-labeled neurons (arrowheads) were found in the surrounding area. Asterisks (*) mark the lesion site in both sections. R: rostral, C: caudal, D: dorsal, V: ventral. Scale bars: A and C = 500 µm, B, B1-2 and D, D1-3 = 20 µm.

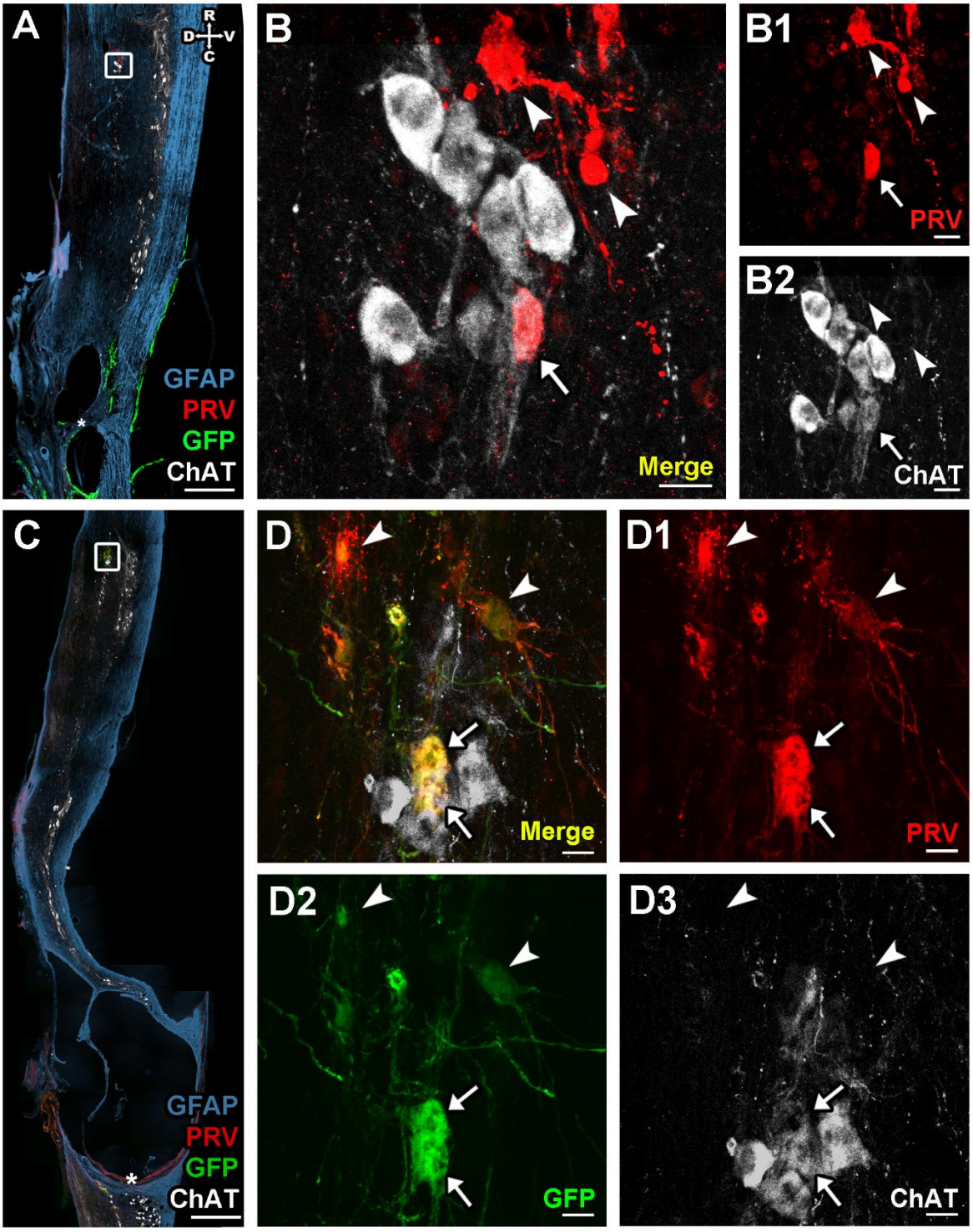
A
R
D
V
C
GFAP
PRV
GFP
ChAT
B
Merge
B1
PRV
B2
ChAT
C
GFAP
PRV
GFP
ChAT
D
Merge
D1
PRV
D2
GFP
D3
ChAT

Figure 9. An incompletely lesioned rat displayed PRV-labeled neurons in the intermediolateral column in the thoracic spinal cord. A. Horizontal section of the T3-T6 spinal cord was processed for RFP-PRV (red), and ChAT-labeled (white) sympathetic preganglionic neurons (SPNs). B, B1-2: Enlargement of box B from A shows that some RFP-PRV-labeled neurons co-express ChAT, consistent with their SPN identity (arrowheads), whereas ChAT is not detected in a nearby PRV-containing cell. C, C1-2: Horizontal section immediately ventral to the section in A, was processed for RFP-PRV (red) and Chx10 (white). Two RFP-PRV neurons (arrows) in the intermediolateral spinal cord co-expressed Chx10, whereas the others were Chx10-negative. R: rostral, C: caudal, L: lateral, M: medial. Scale bars: A = 500 μm, B, B1-2 and C, C1-2 = 100 μm.

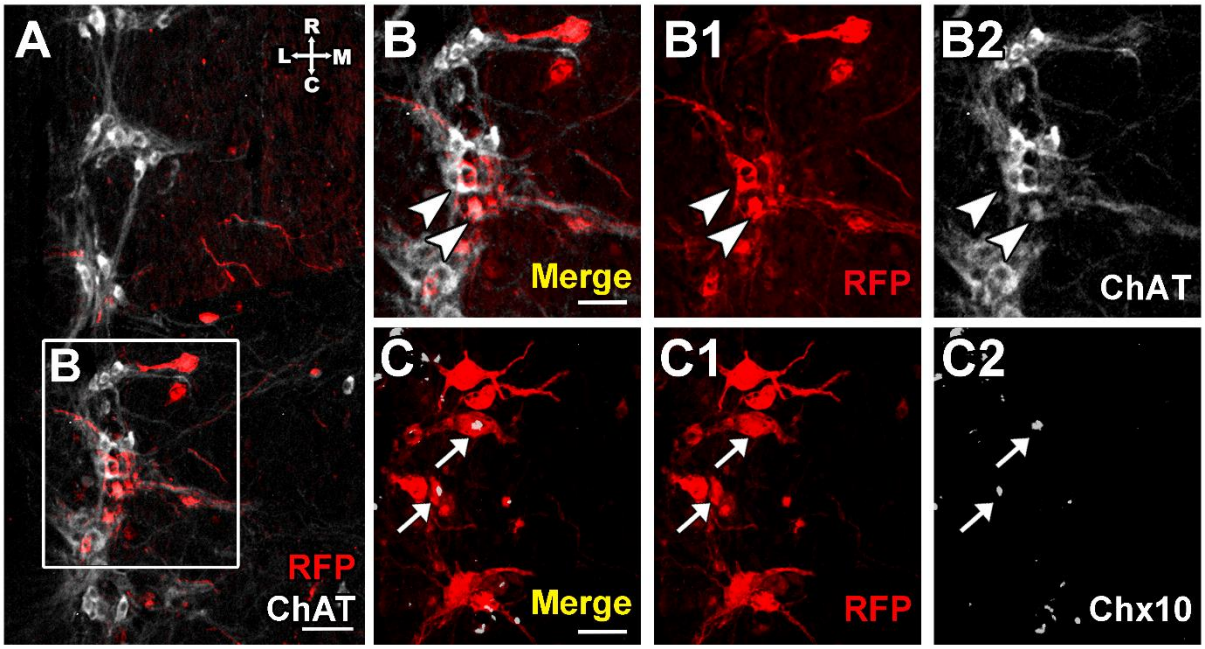
A
R
L
M
C
B
RFP
ChAT
B
Merge
B1
RFP
B2
ChAT
C
Merge
C1
RFP
C2
Chx10

References

Al-Mosawie, A., Wilson, J. M., Brownstone, R. M., 2007. Heterogeneity of V2-derived interneurons in the adult mouse spinal cord. Eur. J. Neurosci., 26, 3003-3015.

Banfield, B. W., Kaufman, J. D., Randall, J. A., Pickard, G. E., 2003. Development of pseudorabies virus strains expressing red fluorescent proteins: New tools for multisynaptic labeling applications. J. Virol., 77, 10106-10112.

Batista, M. F., Lewis, K. E., 2008. Pax2/8 act redundantly to specify glycinergic and GABAergic fates of multiple spinal interneurons. Dev. Biol., 323, 88-97.

Callaway, E. M., 2008. Transneuronal circuit tracing with neurotropic viruses. Curr. Opin. Neurobiol., 18, 617-623.

Card, J. P., Enquist, L. W., 2014. Transneuronal circuit analysis with pseudorabies viruses. Curr. Protoc. Neurosci., Wiley, Hoboken, NJ, 68, 1.5.1-1.5.39.

Courtine, G., Song, B., Roy, R. R., Zhong, H., Herrmann, J. E., Ao, Y., Qi, J., Edgerton, V. R., Sofroniew, M. V., 2008. Recovery of supraspinal control of stepping via indirect propriospinal relay connections after spinal cord injury. Nat. Med., 14, 69-74.

Courtine, G., Gerasimenko, Y., van den Brand, R., Yew, A., Musienko, P., Zhong, H., Song, B., Ao, Y., Ichiyama, R. M., Lavrov, I., Roy, R. R., Sofroniew, M. V., Edgerton, V. R., 2009. Transformation of nonfunctional spinal circuits into functional states after the loss of brain input. Nat. Neurosci., 12, 1333-1342.

Crone, S. A., Quinlan, K. A., Zagoraiou, L., Droho, S., Restrepo, C. E., Lundfald, L., Endo, T., Setlak, J., Jessell, T. M., Kiehn, O., Sharma, K., 2008. Genetic ablation of V2a ipsilateral

interneurons disrupts left-right locomotor coordination in mammalian spinal cord. Neuron, 60, 70-83.

Dougherty, K. J., Kiehn, O., 2010. Firing and cellular properties of V2a interneurons in the rodent spinal cord. J. Neurosci., 30, 24-37.

Edgerton, V. R., Harkema, S., 2011. Epidural stimulation of the spinal cord in spinal cord injury: Current status and future challenges. Expert Rev. Neurother., 11, 1351-1353.

Gad, P., Choe, J., Nandra, M. S., Zhong, H., Roy, R. R., Tai, Y. C., Edgerton, V. R., 2013. Development of a multi-electrode array for spinal cord epidural stimulation to facilitate stepping and standing after a complete spinal cord injury in adult rats. J. Neuroeng. Rehabil., 10, 2.

Gerasimenko, Y., Roy, R. R., Edgerton, V. R., 2008. Epidural stimulation: Comparison of the spinal circuits that generate and control locomotion in rats, cats and humans. Exp. Neurol., 209, 417-425.

Harkema, S., Gerasimenko, Y., Hodes, J., Burdick, J., Angeli, C., Chen, Y., Ferreira, C., Willhite, A., Rejc, E., Grossman, R. G., Edgerton, V. R., 2011. Effect of epidural stimulation of the lumbosacral spinal cord on voluntary movement, standing, and assisted stepping after motor complete paraplegia: A case study. Lancet, 377, 1938-1947.

Hayashi, M., Hinckley, C. A., Driscoll, S. P., Moore, N. J., Levine, A. J., Hilde, K. L., Sharma, K., Pfaff, S. L., 2018. Graded arrays of spinal and supraspinal V2a interneuron subtypes underlie forelimb and hindlimb motor control. Neuron, 97, 869-884.e865.

Hori, K., Hoshino, M., 2012. GABAergic neuron specification in the spinal cord, the cerebellum, and the cochlear nucleus. Neural Plast., 2012, 1-11.

Ichiyama, R. M., Courtine, G., Gerasimenko, Y. P., Yang, G. J., van den Brand, R., Lavrov, I. A., Zhong, H., Roy, R. R., Edgerton, V. R., 2008. Step training reinforces specific spinal locomotor circuitry in adult spinal rats. J. Neurosci., 28, 7370-7375.

Kerman, I. A., Enquist, L. W., Watson, S. J., Yates, B. J., 2003. Brainstem substrates of sympatho-motor circuitry identified using trans-synaptic tracing with pseudorabies virus recombinants. J. Neurosci., 23, 4657-4666.

Khankan, R. R., Griffis, K. G., Haggerty-Skeans, J. R., Zhong, H., Roy, R. R., Edgerton, V. R., Phelps, P. E., 2016. Olfactory ensheathing cell transplantation after a complete spinal cord transection mediates neuroprotective and immunomodulatory mechanisms to facilitate regeneration. J. Neurosci., 36, 6269-6286.

Krassioukov, A. V., Bunge, R. P., Pucket, W. R., Bygrave, M. A., 1999. The changes in human spinal sympathetic preganglionic neurons after spinal cord injury. Spinal Cord, 37, 6-13.

Larsson, M., 2017. Pax2 is persistently expressed by GABAergic neurons throughout the adult rat dorsal horn. Neurosci. Lett., 638, 96-101.

Li, Y., Li, D., Raisman, G., 2005. Interaction of olfactory ensheathing cells with astrocytes may be the key to repair of tract injuries in the spinal cord: The ‘pathway hypothesis’. J. Neurocytol., 34, 343-351.

Mennerick, S., Zorumski, C. F., 2000. Neural activity and survival in the developing nervous system. Mol. Neurobiol., 22, 41-54.

Miles, G. B., Hartley, R., Todd, A. J., Brownstone, R. M., 2007. Spinal cholinergic interneurons regulate the excitability of motoneurons during locomotion. Proc. Natl. Acad. Sci. U.S.A., 104, 2448-2453.

Mondello, S. E., Kasten, M. R., Horner, P. J., Moritz, C. T., 2014. Therapeutic intraspinal stimulation to generate activity and promote long-term recovery. Front. Neurosci., 8, 21.

Ni, Y., Nawabi, H., Liu, X., Yang, L., Miyamichi, K., Tedeschi, A., Xu, B., Wall, N. R., Callaway, E. M., He, Z., 2014. Characterization of long descending premotor propriospinal neurons in the spinal cord. J. Neurosci., 34, 9404-9417.

Phelps, P., Barber, R., Houser, C., Crawford, G., Salvaterra, P., Vaughn, J., 1984. Postnatal development of neurons containing choline acetyltransferase in rat spinal cord: An immunocytochemical study. J. Comp. Neurol., 229, 347-361.

Ramón-Cueto, A., Cordero, M. I., Santos-Benito, F. F., Avila, J., 2000. Functional recovery of paraplegic rats and motor axon regeneration in their spinal cords by olfactory ensheathing glia. Neuron, 25, 425-435.

Rotto-Percelay, D., Wheeler, J., Osorio, F., Platt, K., Loewy, A., 1992. Transneuronal labeling of spinal interneurons and sympathetic preganglionic neurons after pseudorabies virus injections in the rat medial gastrocnemius muscle. Brain Res., 574, 291-306.

Stepien, A. E., Tripodi, M., Arber, S., 2010. Monosynaptic rabies virus reveals premotor network organization and synaptic specificity of cholinergic partition cells. Neuron, 68, 456-472.

Takeoka, A., Jindrich, D. L., Munoz-Quiles, C., Zhong, H., van den Brand, R., Pham, D. L., Ziegler, M. D., Ramon-Cueto, A., Roy, R. R., Edgerton, V. R., Phelps, P. E., 2011. Axon

regeneration can facilitate or suppress hindlimb function after olfactory ensheathing glia transplantation. J. Neurosci., 31, 4298-4310.

Tillakaratne, N. J., Duru, P., Fujino, H., Zhong, H., Xiao, M. S., Edgerton, V. R., Roy, R. R., 2014. Identification of interneurons activated at different inclines during treadmill locomotion in adult rats. J. Neurosci. Res., 92, 1714-1722.

Thornton, M. A., Mehta, M. D., Morad, T. T., Ingraham, K. L., Khankan, R. R., Griffis, K. G., Yeung, A. K., Zhong, H., Roy, R. R., Edgerton, V. R., Phelps, P. E., 2018. Evidence of axon connectivity across a spinal cord transection in rats treated with epidural stimulation and motor training combined with olfactory ensheathing cell transplantation. Exp. Neurol., 309, 119-133.

Weaver, L., Cassam, A., Krassioukov, A., Llewellyn-Smith, I., 1997. Changes in immunoreactivity for growth associated protein-43 suggest reorganization of synapses on spinal sympathetic neurons after cord transection. Neuroscience, 81, 535-551.

Zagoraiou, L., Akay, T., Martin, J. F., Brownstone, R. M., Jessell, T. M., Miles, G. B., 2009. A cluster of cholinergic premotor interneurons modulates mouse locomotor activity. Neuron, 64, 645-662.

Zholudeva, L. V., Karliner, J. S., Dougherty, K. J., Lane, M. A., 2017. Anatomical recruitment of spinal V2a interneurons into phrenic motor circuitry after high cervical spinal cord injury. J. Neurotrauma, 34, 3058-3065.